Title	Operation-State Monitoring and Energization-Status Identification for Underground Power Cables by Magnetic Field Sensing
Author(s)	Sun, X; Chan, G; Sum, CL; Lee, WK; Jiang, L; Pong, PWT
Citation	IEEE Sensors Journal, 2013, v. 13 n. 11, p. 4527-4533
Issued Date	2013
URL	http://hdl.handle.net/10722/185886
Rights	IEEE Sensors Journal. Copyright © IEEE.

Operation-State Monitoring and Energization-Status Identification for Underground Power Cables by Magnetic Field Sensing

Xu Sun, Chun Kit Poon, Geoffrey Chan, Cher Leung Sum, Wing Kin Lee, Lijun Jiang, and Philip W. T. Pong

***Abstract*— In this paper, a novel nondestructive method based on magnetic field sensing is proposed for underground power cable operation-state monitoring and energization-status identification. The magnetic field distribution of the cable is studied using finite element method (FEM) for the power cable operating in different states, i.e., current-energized state (the cable is energized and carries load current) and voltage-energized state (the cable is energized but carries no load current). This innovative method can reconstruct all the source parameters of the cable based on a set of measured magnetic field values. Stochastic optimization technique is applied to realize the reconstruction based on the measured magnetic field. The technology is developed with an artificial immune system algorithm that is able to find out the global optimum with high probability even if very little knowledge about objective function is provided. Application of this method is demonstrated on an 11 kV cable with metallic outer sheath. The results highly match with the actual source parameters of the cable. For application in practice, possible limitations introduced by the nonidealistic of magnetoresistive sensor on magnetic field measurement are discussed and corresponding solutions are suggested. An experimental setup is constructed and the test results are used for the demonstration of this method. This paper shows that the proposed method is able to monitor the operation states of an underground power cable with high accuracy. Engineers can also correctly identify the energization status of the target cable during onsite maintenance. This method is adaptable to other kinds of power cables simply by updating the geometrical and material parameters of the cable in the FEM computation. Moreover, this is an entirely passive method and does not need any active signal injection into the cable.**

***Index Terms*— Magnetic field sensing, underground power cable, operation state, energization status, magnetoresistive sensors, current source reconstruction.**

Manuscript received March 28, 2013; revised May 10, 2013; accepted May 21, 2013. Date of publication May 30, 2013; date of current version October 2, 2013. This work was supported in part by the Seed Funding Program for Basic Research from the University of Hong Kong, the RGC-GRF under Grant HKU 704911P, the University Grants Council of Hong Kong under Contract AoE/P-04/08, and ITF Tier 3 funding under Grant ITS/112/12. The associate editor coordinating the review of this paper and approving it for publication was Prof. Stefan J. Rupitsch.

X. Sun, C. K. Poon, W. K. Lee, L. Jiang, and P. W. T. Pong are with the Department of Electrical and Electronic Engineering, The University of Hong Kong, Hong Kong (e-mail: sunxu@eee.hku.hk; chunkitp@yahoo.com.hk; wklee@eee.hku.hk; jianglj@hku.hk; ppong@eee.hku.hk).

G. Chan and C. L. Sum are with Hongkong Electric Company Ltd., Hong Kong (e-mail: glchan@hkelectric.com; clsum@hkelectric.com).

Color versions of one or more of the figures in this paper are available online at http://ieeexplore.ieee.org.

Digital Object Identifier 10.1109/JSEN.2013.2265305

I. Introduction

UNDERGROUND power cables are commonly used for delivering electricity from distribution networks to customers in metropolises. Operation-state monitoring for underground power cable is required so that engineers can be aware of the cable operation state in time and manage the maintenance to avoid serious power incidents. Besides, very often, onsite works have to be carried out on the underground cable system due to either regular maintenance or unexpected incidents. Correct identification of the target cable from a bundle of power cable for works is an essential task in view of reliability of electricity supply system. Energization-status identification is challenging due to congested underground utility services in almost every part of a major city. Especially for energized cables without load current (i.e. voltage-energized), their energization status are difficult to detect because the detective principle of all the existing cable detection instruments is based on the magnetic field emanated from the load current. It poses a thorny challenge to engineers to identify correctly the target cable before spiking the cable for works. At present, there is no such a method that can realize the above-mentioned functions nondestructively. Some detection methods would damage the cable while others are limited by the characteristics of cable, such as number of conductors and materials [1].

In this work, a novel method based on magnetic field sensing is developed for monitoring the operation-state and identifying the energization-status of underground power cables. Currently, commercially available magnetoresistive (MR) magnetic sensors are widely used which thanks to its sensitivity down to around 10^{-9} Tesla and high spatial resolution of 0.9 mm [2]–[6]. Based on the measured magnetic field, the engineers can find out the cable operation state and obtain its electrical information in real time. When work is carried out on the target cable, this technology can be used to find out the energization status of the target cable before spiking the cable and thus it guarantees the safety of engineer and electricity supply to customers will not be interrupted.

The content of this paper is as follows: first, numerical method is used to study the magnetic field of energized cable. The relation between magnetic field distribution and cable operation states is analyzed, and the measurement method by using magnetoresistive (MR) sensors is described. The

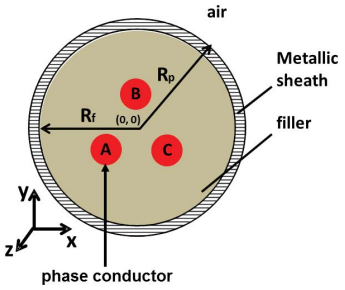

Fig. 1. The geometrical configuration of BS6622 pipe-type underground power cable. The symbol A, B, and C denote the phase conductors.

voltage-energized target cable can be recognized by a certain pattern of a set of measured magnetic field values. For energized cables with load current (i.e. current-energized), a stochastic optimization technique is developed and applied to reconstruct the unknown current source parameters from the measured magnetic field reversely. The operation state of the cable can be derived by analyzing the parameters of the reconstructed current sources. Finally, the application of this method is demonstrated on an experimental setup. The reconstruction results on different cable operation states are provided with error analysis. The potential pitfalls due to MR sensor non-idealities on magnetic detection in the actual environment are considered and discussed.

II. The Magnetic Field of Underground Powercable

Finite element method (FEM) is widely used to create the electromagnetic model of different types of power cable [7]–[9]. In these reported works, efforts were made to validate the numerical results by comparing with measured data and good agreements were obtained. In this paper, a BS6622a three-core 11 kV power cable (rated phase current $I_i = 540$ A, $\phi_A = -120°$, $\phi_B = 0°$, $\phi_C = 120°$) is chosen to be the demonstration example, and FEM was used to study the magnetic field in and around this type of cable. The FEM approach is taken rather than the analytical approach so that this method can be easily adapted to another kind of cable just simply by updating the geometrical and material parameters in the FEM model, as opposed to deriving the analytical solution from scratch again which may not be possible sometimes. The detailed geometrical, material, electrical and electromagnetic parameters of the cable can be found in [10]. A simplified electromagnetic modal of the cable is illustrated in Fig. 1. In the model, the three-conductor cores are arranged symmetrically with fillers whose radius is R_f. They are enclosed by a metallic outer sheath (outer radius is R_p) insulated with dielectric. The boundary of the electromagnetics model is at $r = R_a$. A homogeneous Dirichlet boundary condition that $A_z = 0$ is imposed on $r = R_a$. The electromagnetic characteristic of each region of the cable is described by the material relative permittivity, conductivity and relative permeability as listed in Table I. Before computing the magnetic field of the power cable, the following assumptions are made:

1) the phase currents $I_i (i = A, B, C)$ flowing in the phase conductors are only along the conductor, which is z-direction in this paper. They result in z-direction magnetic vector potential A_z;
2) the permeability of the metallic sheath is constant;
3) the conductivities of the conductors and metallic sheath are constant;
4) the displacement currents are neglected when the cable is current-energized.

TABLE I
Electromagnetic Properties of the Material of the Cable and Surrounding Medium

	ε_r	σ_r (s/m)	μ_r
Phase conductor (Copper)	1.0	5.8×10^7	1.0
Conductor insulator (XLPE)	2.3	0.0	1.0
Filler (Polypropylene)	2.3	0.0	1.0
Metallic sheath (Copper)	1.0	5.8×10^7	1.0
Air	1.0	0.0	1.0

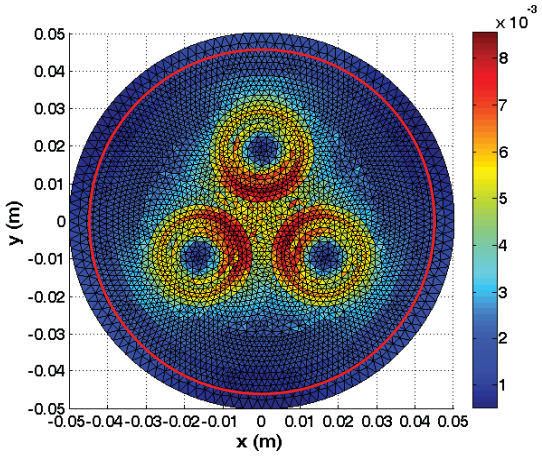

Fig. 2. Simulated magnetic field when the cable is current-energized. The color bar denotes the magnitude of magnetic flux density vector. The red circle denotes the surface of the power cable.

Derived from Maxwell's equations, we formulated and solved the differential equations with A_z as variable, in each region of the model with similar steps as in [7]. For the current-energized scenario, the finite element mesh structure of the model and the computed magnitude of magnetic field flux density are shown in Fig. 2. It is shown that the maximum magnetic field is 1.5 milliTesla in the vicinity of each of the phase conductors while the minimum value is 0.5 milliTesla on the cable surface. The field distribution is changed correspondingly when the phase current variation happens. For example, when there is a +15% imbalance of current magnitude in phase A conductor, the magnetic field on the cable surface is changed correspondingly as shown in Fig. 3. The magnetic field surrounding the cable surface under this +15% imbalance condition is denoted by the dash

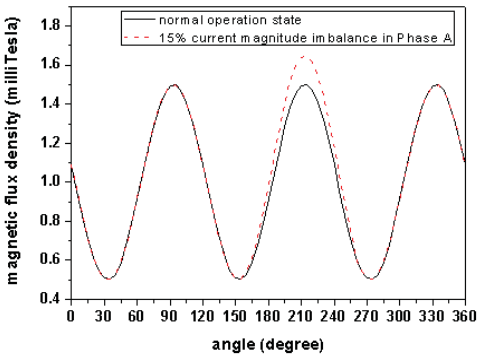

Fig. 3. Simulated magnetic field (dash curve) on cable surface when there is +15% current amplitude imbalance in phase A. The solid curve denotes the magnetic field under normal operation state.

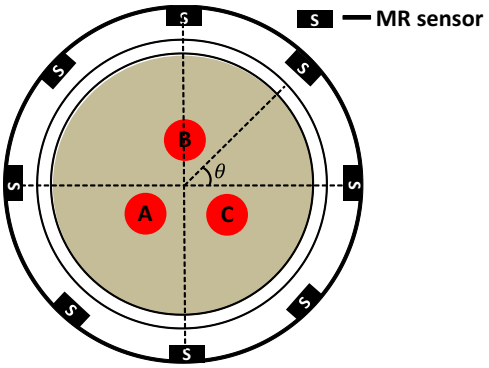

Fig. 4. The positions of MR sensors that are used to sense the magnetic field around the voltage-energized cable surface. The A, B, and C denote the phase conductors.

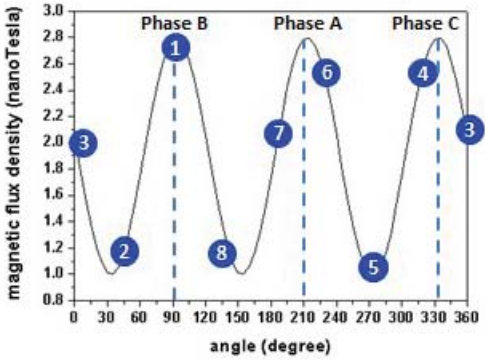

Fig. 5. Simulated magnetic field around the voltage-energized cable surface.

line whereas the solid line denotes the magnetic field under normal operation state. It is found that the maximum magnetic field increases to 1.64 milliTesla on the cable surface in the vicinity of the phase A conductor due to its +15% current imbalance.

For the voltage-energized scenario, since the cable outer metallic sheath (neutral conductor) and the phase conductors are separated with the filler insulator, the cable can be considered as a capacitor. When it is energized without load (voltage-energized), one can expect that charging current is still present and it depends on the cable capacitance. The charging current is a kind of displacement current which is the effect of the charge density variation on the phase conductors and the metallic sheath. The charging current is considered as phase current and assumed to flow in the sheath along axis direction that [7]

$$\sum_{i}^{i=A,B,C} I_i = I_p \tag{1}$$

where the I_i is charging current flowing in phase conductor and the I_p is the metallic sheath current in axis direction. When these current sources are imposed, the magnetic field can be deduced by solving the differential equations of A_z. If we define a set of equally separated field points as MR sensor positions around the cable surface, as shown in Fig. 4, groups of measured data are available for observing the magnetic field of the voltage-energized power cable. The azimuth θ is used to denote the position on the cable surface. Fig. 5 shows the magnetic field distribution around the surface of the voltage-energized cable. The positions of the eight measuring points on the cable surface are located in the figure. It is found that the magnetic field generated by the charging current varies from 2.8 nanoTesla to 1.0 nanoTesla in the form of a sinusoid. The maximum values (2.8 nanoTesla) are obtained on the cable surface in the vicinity of each of the inner phase conductors at the angles of 210° (phase A), 90° (phase B), and 330° (phase C). When this specific pattern of magnetic field is detected by the sensor array placed around the cable surface, we can determine that the target cable is voltage-energized. It should be noted that since the charging current is proportional to the length of the cable, its value is much higher than the rating value of unit length (1.05 mA) in a practical cable and the emanated magnetic signal is also larger [10]. For a 100 m cable, the charging current would be 105 mA and its emanated magnetic signal would be 100 times larger. Thus energization-status discrimination would be even easier in the actual scenario.

III. Source Reconstruction Methodology

Based on the knowledge of the magnetic field of the power cable, it is found that the cable energization status and the current sources determine the distribution of the emanated magnetic field. In the scenario of energization-status identification, the voltage-energized cable can be identified from the amplitude and distribution pattern of the measured magnetic field as described in the previous section. In the scenario of operation-state monitoring, it requires obtaining the electrical information of the power cable, such as current amplitude, frequency, and phase angle, which can be found by reconstructing the current sources reversely from the magnetic field. Optimization techniques can be used to undertake the task of source reconstruction based on the magnetic field. If the knowledge of objective function behavior is provided, for example a global minimum exists in a local region, deterministic optimization methods converge very fast to the objective function's solution. However, if the knowledge of the objective function behavior is unavailable in the multidimensional parameter space, a stochastic strategy is preferred because it is more likely to find out the global optimum. In this method,

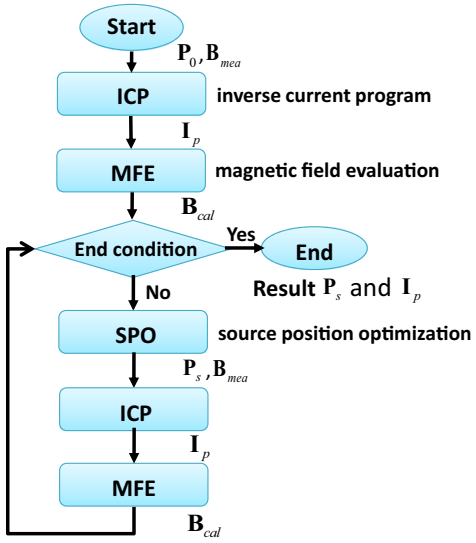

Fig. 6. Flowchart of current source reconstruction from magnetic field sensing.

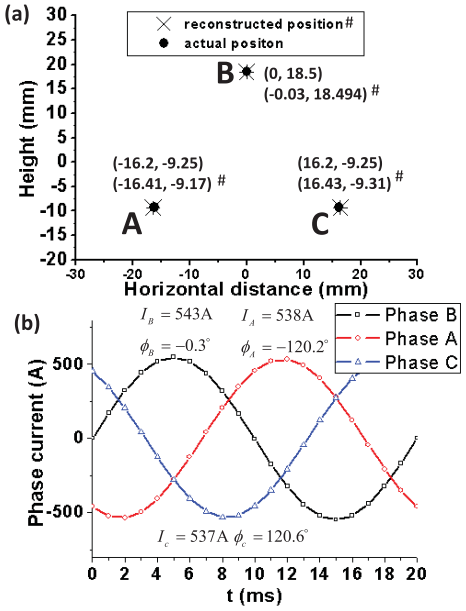

Fig. 7. Results of current source reconstruction for the current-energized cable in Fig. 2. (a) Actual and reconstructed positions of phase conductors, (b) reconstructed phase current curve of each phase conductor.

the optimization is operated on both the phase currents and positions of the cable conductors. Two algorithms including least square approximation (LSA) and artificial immune system (AIS) are used to identify the unknown parameters [11]. The optimization process is described in the flowchart (Fig. 6). It starts with a group of default position parameters $\mathbf{P}_0$ of the cable conductors. Phase current $\mathbf{I}_p$ in each conductor is calculated by the inverse current program (ICP), which is based on the LSA algorithm with position parameters and measured magnetic field $\mathbf{B}_{\text{mea}}$ as variables by this equation,

$$\mathbf{I}_p = (\mathbf{A}^T\mathbf{A})^{-1}\mathbf{A}^T\mathbf{B}_{\text{mea}} \tag{2}$$

where $\mathbf{A}$ is the coefficient matrix which depends on the configuration of current source positions. Then the magnetic field $\mathbf{B}_{\text{cal}}$ is computed by inputting $\mathbf{I}_p$ and configuration parameters $\mathbf{A}$ into the magnetic field evaluation (MFE) module based on FEM analysis as

$$\mathbf{B}_{\text{cal}} = \mathbf{A}\mathbf{I}_p. \tag{3}$$

There is a predetermined minimum threshold value of the Euclidean distance $\|\mathbf{B}_{\text{cal}} - \mathbf{B}_{\text{mea}}\|$ as the end condition for terminating the optimization loop. If the end condition is not satisfied, the algorithm will randomly generate a new group of position parameters $\mathbf{P}_s$ by using the AIS algorithm in the source position optimization (SPO) module. With the $\mathbf{B}_{\text{mea}}$ and the generated $\mathbf{P}_s$, the $\mathbf{I}_p$ is calculated again in the ICP module. The $\mathbf{P}_s$ and new $\mathbf{I}_p$ are then used to compute new $\mathbf{B}_{\text{cal}}$ by FEM analysis in the MFE. Then the Euclidean distance between the calculated $\mathbf{B}_{\text{cal}}$ and $\mathbf{B}_{\text{mea}}$ is found again and compared with the minimum threshold. If the Euclidean distance is smaller than the minimum threshold value, the whole optimizing process is finished, and then the resulting $\mathbf{P}_s$ and $\mathbf{I}_p$ are adopted as the optimum current source parameters; otherwise, the iteration continues. This optimization process is repeated multiple times (N) to obtain N sets of optimum current source parameters. The final $\mathbf{P}_s$ are the ensemble averages of these N sets of optimum values. Accordingly, the final $\mathbf{I}_p$ can be obtained from the final $\mathbf{P}_s$ and the measured magnetic field.

IV. Simulation Results and Experimental Proof

Figure. 7(a) shows the results of the reconstructed conductor positions of the current-energized scenario described in Fig. 2, where the cable center is at (0, 0) and the actual positions of the phase conductor centers are A (−16.2, −9.25), B (0, 18.5), and C (16.2, −9.25). The actual and reconstructed positions are marked in the Fig. 7(a). The average error of the reconstruction is less than 0.30 mm which is 0.25% of the cable diameter. The value of each phase current is reconstructed at every 1 ms during a complete current cycle (20 ms). The results are shown in Fig. 7(b). The reconstructed current cycle is found to be 20.14 ms, corresponding to a system frequency of 49.7 Hz with a small error of 0.6% from the rated frequency 50 Hz. The reconstructed current amplitudes in phase A, B, and C are 538A, 543A, and 537A respectively. These are only slightly deviated from the actual amplitude of 540 A by less than 0.6%. The reconstructed phase angles in phase A, B, and C are −120.2°, −0.3°, and 120.6° respectively. These values are merely deviated from the actual angles by less than 0.5%. These reconstructed results provide the engineers with the operation state of the cable, and they can realize that the cable is under normal operation state in this case. Fig. 8 shows the reconstructed results of the +15% current imbalance scenario described in Fig. 3. The reconstructed and the actual conductor positions are shown in Fig. 8(a). The average error of the reconstructed positions is only 0.26 mm which is 0.22% of the cable diameter. The reconstructed results of the phase currents are shown in Figure. 8(b). The reconstructed current cycle is found to be 20.11 ms, corresponding to a system frequency of 49.73 Hz

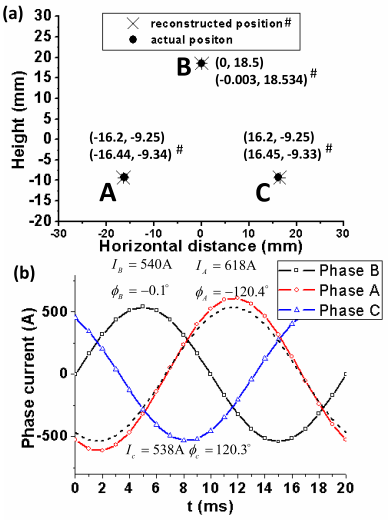

Fig. 8. Results of current source reconstruction when +15% current imbalance happens in phase A in Fig. 3. (a) Actual and reconstructed positions of phase conductors, (b) reconstructed phase current curve of each phase conductor. Dash line denotes the current curve when no current imbalance happens in phase A.

with a small error of 0.54% from the rated frequency 50 Hz. The reconstructed current amplitude of phase A is 618 A which correctly traces the +15% current imbalance (with an error less than 0.5%). The results show that there is phase current overload in phase conductor A. These reconstructed results enable the engineers to observe whether the operation state of the power cable is abnormal and appropriate remedial action can be immediately taken. To a greater extent, since this method is capable of detecting the abnormal situation of phase current overload, the control center can diagnose that the system is operating in unstable states. The method can also provide the information of system frequency. The frequency can be observed by reading the current cycle such as in Fig. 8(b). Since the frequency is a parameter showing the relation between the generation and load, the result can be used to analyze the balance of the power system. In principle, this method can also detect current phase angle imbalance. The current phase angle imbalance would be manifested as a horizontal shift of phase current curve in the reconstruction. The imbalance in phase current angle can indicate the fault occurrence.

In order to evaluate the practicality of this novel method based on MR sensors, it is necessary to discuss the effects of MR sensor non-idealities on magnetic detection and provide corresponding solutions. According to our FEM simulation results, the magnetic field generated by a current-energized three-phase underground cable (typically carrying hundreds ampere of current) is on the order of milliTesla. When the cable is voltage-energized, the generated magnetic signal is much weaker because the rated charging current is much smaller than the rated phase current, and it is calculated to be on the order of nanoTesla. Therefore, the effects of MR sensor non-idealities (offset, hysteresis, and 1/f noise) should be considered for obtaining accurate magnetic field measurement. Technical approaches are available for canceling the effects of MR sensor non-idealities. For example, the hysteresis can be reduced by applying an external magnetic field in the direction of hard axis [12]. The offset drift with temperature in MR sensor can be canceled by a temperature compensation circuit. The effect of temperature on the MR sensors can be predetermined and then the temperature compensation circuit can be designed to rectify the temperature drift [13]. 1/f noise has been reduced to a low level in recent commercial MR sensors, which can reach a detectability of 3 nT/Hz$^{1/2}$ at 10 Hz. Since the 1/f noise decreases with the frequency, TMR sensors (such as STJ-301 manufactured by Micro Magnetics [14]) has detectability better than 3 nT at 50 Hz with noise level below 1 nT. They can be used to obtain information from the voltage-energized cables. Thus, the sensitivities of MR sensors are good enough for sensing the magnetic field emanated from the underground power cable in different operation states and energization status. We can obtain accurate current reconstruction results based on the measured magnetic field data. In addition, since the cross-section dimension of a power cable is typically only about a few tens of millimeter in radius (40 mm for BS6622a cable), this requires a compact sensor which allows an array of them to be placed around the cable in order to sense the magnetic field at multiple points on the cable surface. The more field point data, the more accurate the reconstructed current sources. Since MR sensors are much smaller in size than other traditional magnetic field sensors, such as Hall sensors and fluxgate sensors, we can place a MR sensor array surrounding the cable surface to obtain a group of magnetic field data. The sensor array can measure the cable magnetic field with very high spatial resolution down to 0.9 mm with some commercially available MR sensors [9].

In order to verify this monitoring technology, a laboratory setup including MR three-axis sensor (Honeywell HMC2003) array and 11 kV three-phase underground power cable was established in the Smart Grid and High Power System Laboratory of The University of Hong Kong. The cross-section of the cable used in the experiment is shown in Fig. 9(a). The MR sensors are equally separated and surrounding the cable surface (Fig. 9(b)) to measure magnetic field vectors with high sensitivity. When power supply was connected with the cable through the conductors, amplitudes of the measured phase currents were 16.1 A, 16.3 A and 15.7 A in phase A, B and C respectively. The magnetic field was measured by the MR sensors at a rotation step of 10 degree around the cable surface. The rotation angle θ in Fig. 10 is the same as the azimuth θ in Fig. 4. As shown in Fig. 10, the measured and simulated magnetic field results are compared. The measured results coincide well with the simulation except for the region near phase conductor C. As can be observed from Fig. 9(a), each phase conductor is composed of a bunch of copper filaments which are bound together. Structural flaw during manufacturing may cause the uneven distribution of the electrical resistance in the conductor phase C, making the cross-section of the conductive path no longer a perfect circular shape that significantly affects the magnetic field distribution nearby phase conductor C. As shown in Fig. 4, the magnetic field is measured at the eight field points to reconstruct the operation state of this

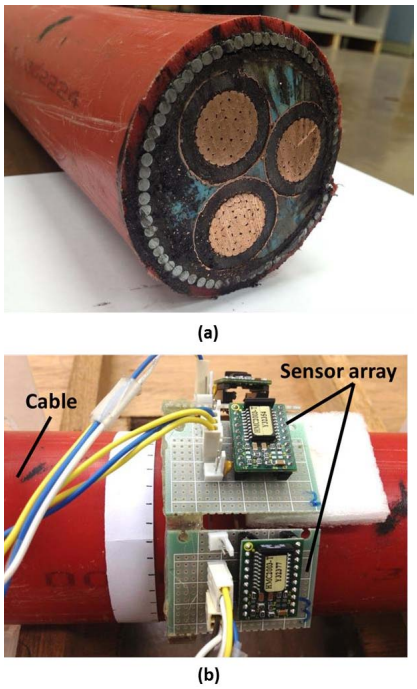

Fig. 9. Experimental setup. (a) Cross-section of the power cable, (b) MR sensor array installed on the cable surface.

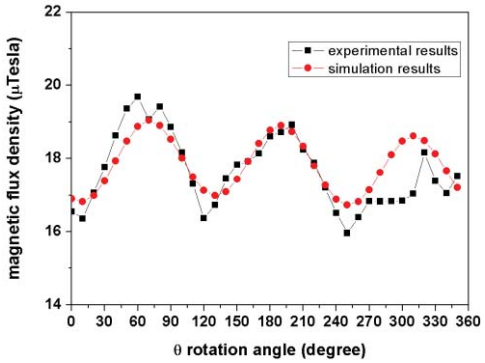

Fig. 10. Measured and simulated magnetic field on the cable surface.

power cable. The construction results of conductor positions (A (−16.03, −9.28), B (0, 18.46), and C (15.02, −8.23)) are shown in Fig. 11(a). The error of the reconstruction for conductor A and B is less than 0.2 mm. The reconstructed position of conductor C slightly deviates from the actual conductor center by 1.537 mm which is ascribed to the imperfect conductive path of conductor C and thus distorted magnetic field distribution. The values of reconstructed phase currents during a complete current cycle (20 ms) are shown in Fig. 11(b). The reconstructed current amplitudes in phase A, B, and C are 16.0 A, 16.33 A, and 15.66 A respectively. The difference between these reconstructed current amplitudes and the actual measured amplitude is less than 0.625%. The reconstructed phase angles in phase A, B, and C are −120.07°, −0.3°, and 120.03° respectively with error less than 0.25%. The reconstructed current cycle is found to be 20.1 ms, corresponding to a system frequency of 49.75 Hz with a small error of 0.5% from the rated frequency 50 Hz. In general, the reconstructed electrical and geometrical parameters agree

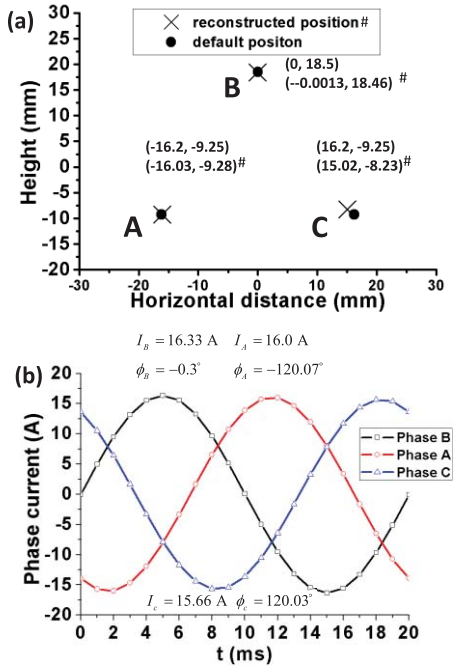

Fig. 11. Results of current source reconstruction from the measured magnetic field. (a) Reconstructed positions of phase conductors and the actual conductor centers of the cable, (b) reconstructed phase current curve of each phase conductor.

very well with the actual values. Their average deviations are typically less than 3.0% in geometry and 0.625% in phase currents.

V. Conclusion

This work aims at developing a method for identifying the energization status and monitoring the operation state of underground power cables based on magnetic field sensing. The relations between the emanated magnetic field and the cable operation states were studied by FEM simulation. When the cable is voltage-energized, the energization status of the target cable can be determined based on the specific pattern of the emanated magnetic field due to the charging current. When the cable is current-energized, stochastic optimization technique is applied to reconstruct the current source parameters inversely. To validate the method, issues introduced by the MR sensor non-idealities in magnetic field measurement are considered and solutions are suggested. It demonstrates that engineers can monitor the cable operation states from the measured magnetic field and identify correctly the energization status for works. From the experiments, the reconstructed results calculated from the magnetic field measured by the MR sensors match very well with the actual electrical and geometrical values of the cable. Even though there are unavoidable imperfection in the setup and non-idealities in the sensors, the proposed technique can accurately provide the electrical and geometrical information of the power cable with just tiny error. As such, this method is promising for monitoring the underground power cable and providing the electrical information of the target cable for engineers. It has great potential to enable dynamic line rating and realize real-time monitoring for the

future Smart Grid. Its ability to correctly identify the voltage-energized status of a cable is an important breakthrough in cable detection technology that can assist site engineers to identify target cable correctly, avoiding unnecessary power supply interruption and ensuring safety of workers. Although this method is demonstrated on a BS6622a cable in this study, it should be reiterated that it is universally applicable for a variety of power cables by updating the FEM model with the geometrical and material parameters of the specific type of cable.

REFERENCES

[1] S. X. Short, A. V. Mamishev, T. W. Kao, and B. D. Russell, "Evaluation of methods for discrimination of energized underground power cables," *Electr. Power Syst. Res.*, vol. 37, pp. 29–38, Apr. 1996.

[2] T. Chady, "Evaluation of stress loaded steel samples using GMR magnetic field sensor," *IEEE Sensors J.*, vol. 2, no. 5, pp. 488–493, Oct. 2002.

[3] E. Zimmermann, A. Verweerd, W. Glaas, A. Tillmann, and A. Kemna, "An AMR sensor-based measurement system for magnetoelectrical resistivity tomography," *IEEE Sensors J.*, vol. 5, no. 2, pp. 233–241, Apr. 2005.

[4] S. C. Mukhopadhyay, K. Chomsuwan, C. P. Gooneratne, and S. Yamada, "A novel needle-type SV-GMR sensor for biomedical applications," *IEEE Sensors J.*, vol. 7, no. 3, pp. 401–408, Mar. 2007.

[5] M. D. Cubells-Beltran, C. Reig, D. R. Munoz, S. I. P. C. de Freitas, and P. J. P. de Freitas, "Full wheatstone bridge spin-valve based sensors for IC currents monitoring," *IEEE Sensors J.*, vol. 9, no. 12, pp. 1756–1762, Dec. 2009.

[6] E. Sifuentes, O. Casas, and R. Pallas-Areny, "Wireless magnetic sensor node for vehicle detection with optical wake-up," *IEEE Sensors J.*, vol. 11, no. 8, pp. 1669–1676, Aug. 2011.

[7] X. B. Xu and G. Liu, "A two-step numerical solution of magnetic field produced by ELF sources within a steel pipe-Abstract," *J. Electromagn. Waves Appl.*, vol. 14, no. 4, pp. 523–524, 2000.

[8] X. B. Xu and G. H. Liu, "Investigation of the magnetic field produced by unbalanced phase current in an underground three-phase pipe-type cable," *Electr. Power Syst. Res.*, vol. 62, pp. 153–160, Jun. 2002.

[9] X. B. Xu, G. H. Liu, and P. Chow, "A finite-element method solution of the zero-sequence impedance of underground pipe-type cable," *IEEE Trans. Power Del.*, vol. 17, no. 1, pp. 13–17, Jan. 2002.

[10] (2012, Sep. 10). *BS6622/BS7835 11 kV Three Core Power Cable* [Online]. Available: http://www.bbccable.com

[11] P. G. Alotto, C. Eranda, B. Brandstatter, G. Furntratt, C. Magele, and G. Molinari, "Stochastic algorithms in electromagnetic optimization," *IEEE Trans. Magn.*, vol. 34, no. 5, pp. 3674–3684, Sep. 1998.

[12] X. Liu, C. Ren, and G. Xiao, "Magnetic tunnel junction field sensors with hard-axis bias field," *J. Appl. Phys.*, vol. 92, no. 8, pp. 4722–4725, 2002.

[13] J. S. Moreno, D. R. Munoz, S. Cardoso, S. C. Berga, A. E. N. Anton, and P. J. P. de Freitas, "A non-invasive thermal drift compensation technique applied to a spin-valve magnetoresistive current sensor," *Sensors*, vol. 11, pp. 2447–2458, Mar. 2011.

[14] (2012, Jan. 10). *Micromagnetics* [Online]. Available: http://www.micromagnetics.com/

Xu Sun received the B.S. degree from the Northeast China Institute of Electric Power, Jilin, China, in 2005, the M.S. degree from the University of Electronic Science and Technology, Chengdu, China in 2008, and he is currently pursuing the Ph.D. candidate in the Department of Electrical and Electronic Engineering with the University of Hong Kong, Hong Kong. His current research interests include electromagnetics, computational electromagnetics, stochastic optimization, application of magnetoresistive sensor in power system and electric power transmission monitoring.

Chun Kit Poon received the B.S. degree in the School of Science from Hong Kong University of Science and Technology, Hong Kong, in 2012. He is a Research Assistant in the Department of electrical and electronic engineering with the University of Hong Kong.

Geoffrey Chan received the B.Sc. degree in engineering from the University of Hong Kong, in 1977, the M.Sc. degree in information systems, and the M.A. degree in professional English in 1992 and 2006 respectively. He is currently the Chief Technical Services Engineer in the Technical Services Department of the Transmission and Distribution Division from the Hongkong Electric Company Limited, Hong Kong.

Cher Leung Sum received the B.Sc. degree in engineering from the University of Hong Kong, in 1980 and the M.Sc. degree in electrical engineering from the University of New South Wales, New South Wales, Australia. He is currently the Area Engineer in the Construction & Maintenance Department of the Transmission and Distribution Division of the Hongkong Electric Company Limited.

Wing Kin Lee received the B.Sc. degree, the M.Sc. degree from the University of Hong Kong, in 1976 and 1988, respectively, and the M.B.A. degree from the Chinese University of Hong Kong in 1990. He is a professional in electrical services and power engineering, and currently as a Senior Teaching Consultant in the University of Hong Kong. He earned industrial experience while involved with power and communication utility companies in Hong Kong. His current research interests include smart grid demand side management, electrical load signature, and vertical transportation.

Lijun Jiang (S'01–M'04–SM'13) received the B.S. degree from the Beijing University of Aeronautics and Astronautics, Beijing, China, in 1993, the M.S. degree from Tsinghua University, Tsinghua, China, in 1996, and the Ph.D from the University of Illinois, IL, USA, in 2004. Since 2004, he has been a Post-doctoral Researcher, the Research Staff Member, and the Senior Engineer with IBM T.J. Watson Research Center, Cambridge, MA, USA. Since 2009, he has been an Associate Professor in electrical and electronic engineering with the University of Hong Kong. His current research interests include electromagnetics, computational electromagnetics, IC signal/power integrity, IC EMC/EMI, antennas, multidisciplinary EDA solutions, RF and microwave technologies, high performance computing, etc.

Philip W. T. Pong (SM'13) received the Ph.D. degree in engineering from the University of Cambridge in 2005. He has been a Post-doctoral Researcher in the Magnetic Materials Group with the National Institute of Standards and Technology for three years. In 2008, he joined the University of Hong Kong at engineering faculty as an Assistant Professor working on tunneling magnetoresistance sensors, the application of magnetoresistive sensors in smart gridis a physicist, electrical engineer working on magnetoresistive magnetic field sensors, and smart grid with the Department of Electrical and Electronic Engineering, the University of Hong Kong.